An approximate stochastic dynamics approach for design spectrum based response analysis of nonlinear structural systems with fractional derivative elements

Ioannis A. Kougioumtzoglou [*a], Peihua Ni[b], Ioannis P. Mitseas[c,d], Vasileios C. Fragkoulis [b], and Michael Beer[b,e,f]

[a]*Department of Civil Engineering and Engineering Mechanics, Columbia University, USA*
[b]*Institute for Risk and Reliability, Leibniz University Hannover, Germany, E-mail: peihua.ni@irz.uni-hannover.de, fragkoulis@irz.uni-hannover.de, beer@irz.uni-hannover.de.*
[c] *School of Civil Engineering, University of Leeds, UK, E-mail: I.Mitseas@leeds.ac.uk.*
[d]*School of Civil Engineering, National Technical University of Athens, Greece.*
[e]*Institute of Risk and Uncertainty, University of Liverpool, UK.*
[f]*International Joint Research Center for Resilient Infrastructure & International Joint Research Center for Engineering Reliability and Stochastic Mechanics, Tongji University, China*

Abstract

A novel approximate approach is developed for determining, in a computationally efficient manner, the peak response of nonlinear structural systems with fractional derivative elements subject to a given seismic design spectrum. Specifically, first, an excitation evolutionary power spectrum is derived that is compatible with the design spectrum in a stochastic sense. Next, relying on a combination of

---

[*]Corresponding author: ikougioum@columbia.edu

statistical linearization and stochastic averaging yields an equivalent linear system (ELS) with time-variant stiffness and damping elements. Further, the values of the ELS elements at the most critical time instant, i.e., the time instant associated with the highest degree of nonlinear/inelastic response behavior exhibited by the structural system, are used in conjunction with the design spectrum for determining approximately the nonlinear system peak response displacement. The herein developed approach can be construed as an extension of earlier efforts in the literature to account for fractional derivative terms in the governing equations of motion. Furthermore, the approach exhibits the significant novelty of exploiting the localized time-dependent information provided by the derived time-variant ELS elements. Indeed, the values of the ELS stiffness and damping elements at the most critical time instant capture the system dynamics better than an alternative standard time-invariant statistical linearization treatment. This leads to enhanced accuracy when determining nonlinear system peak response estimates. An illustrative numerical example is considered for assessing the performance of the approximate approach. This pertains to a bilinear hysteretic structural system with fractional derivative elements subject to a Eurocode 8 elastic design spectrum. Comparisons with pertinent Monte Carlo simulation data are included as well, demonstrating a high degree of accuracy.

1   Introduction

Contemporary seismic codes favor design spectrum based response analyses of building structures. In this regard, the input seismic action is defined through elastic design spectra that provide the peak response of linear single-degree-of-freedom (SDOF) oscillators as a function of their natural period T and damping ratio ζ (e.g., Chopra [2001]). These are developed, typically, for a nominal damping ratio $\zeta = 0.05$ and are complemented with damping adjustment factors in case a different damping ratio needs to be considered (e.g., Lin et al. [2005]). Nevertheless, seismic codes and regulatory agencies allow ordinary structures to exhibit nonlinear/inelastic response behaviors towards achieving cost-effective designs (e.g., CEN [2004]). In this setting, the problem of estimating the peak nonlinear/inelastic system response subject to a given elastic design spectrum arises naturally in code-compliant

2

structural design applications, and remains a persistent research challenge in the field of earthquake engineering.

Irrespective of the nonlinearity type, the above problem can be addressed by performing nonlinear system response time-history analyses in a Monte Carlo simulation (MCS) context. Specifically, the nonlinear system is subjected to an ensemble of ground motion records, whose average design spectrum matches approximately the target one provided by the codes (e.g., Katsanos et al. [2010]). Such design spectrum compatible excitation records can comprise artificial accelerograms and/or judiciously selected records from relevant databanks (e.g., Giaralis and Spanos [2009], Cacciola [2010], Araújo et al. [2016]). In many cases, these records need to be further scaled and modified to achieve the desired compatibility with the given design spectrum. Note, however, that the operation of scaling accelerograms has raised significant concerns in the literature from a theoretical perspective (e.g., Grigoriu [2011]). Further, to reduce the variability of the peak response data obtained based on the minimum number of accelerograms allowed by the seismic codes (e.g., Beyer and Bommer [2007]), a relatively large number of excitation records are required for the system response analysis. In this manner, numerical integration of the nonlinear equations of motion needs to be performed in MCS fashion; thus, rendering the approach computationally demanding.

Obviously, the aforementioned computational cost becomes higher with increasing complexity of the mathematical model representing the nonlinear/hysteretic system under consideration. In this regard, the need for more accurate modeling of viscoelastic material behavior has led recently to the utilization of advanced mathematical tools such as fractional calculus (e.g., Makris [1997], Sabatier et al. [2007], Rossikhin and Shitikova [2010], Di Paola et al. [2013]). Indeed, models based on fractional derivatives have exhibited a high degree of accuracy compared with experimental viscoelastic response data obtained via creep and relaxation tests. Notably, in contrast to traditional models that utilize combinations of Maxwell and/or Kelvin elements and depend on several parameters, the fractional derivative model requires the identification of two parameters only for capturing both relaxation and creep tests (e.g., Di Paola et al. [2011]). Remarkably, structural engineering has benefited significantly from exploiting fractional calculus concepts. In fact, several research efforts pertaining to seismic isolation and vibration control applications have demonstrated the capability of fractional derivatives to model successfully the response behavior of viscoelastic dampers,

e.g., Koh and Kelly [1990], Makris and Constantinou [1991], Lee and Tsai [1994], Shen and Soong [1995], Rüdinger [2006]. The interested reader is also directed to Petromichelakis et al. [2021] for a recent paper referring to fractional derivative modeling of the capacitance term in the governing equations of a broad class of nonlinear electromechanical energy harvesters. It is noted that solving numerically the corresponding fractional differential equation of motion can be a highly demanding task computationally. This is due to the need for treating numerically the convolution integral associated with the fractional derivative operator in conjunction with complex nonlinearities and hysteresis. In this context, various solution schemes have been developed for determining the response of deterministically and/or stochastically excited nonlinear oscillators with fractional derivative elements (e.g., Koh and Kelly [1990], Spanos and Evangelatos [2010], Di Matteo et al. [2014], Fragkoulis et al. [2019], Pirrotta et al. [2021], Kong et al. [2022a,b]).

It is readily seen that there is merit in developing alternative, more efficient, approaches for treating the problem of estimating the peak response of a nonlinear/hysteretic system with fractional derivative elements subject to a given elastic design spectrum. In this regard, a rather popular class of approaches relates to deriving an equivalent linear system (ELS) based on various deterministic or stochastic linearization criteria (e.g., Iwan [1980], Iwan and Gates [1979a], Jennings [1968], Iwan and Gates [1979b], Hadjian [1982], Koliopulos et al. [1994], Giaralis and Spanos [2010], Mitseas et al. [2018], Mitseas and Beer [2019]). Further, the ELS is characterized by effective stiffness and damping elements that can be used in conjunction with the elastic design spectrum for estimating approximately the peak response of the original system.

In this paper, an approximate stochastic dynamics approach is developed for determining the peak response displacement of nonlinear structural systems with fractional derivative elements subject to a given seismic design spectrum. This is done in a computationally efficient manner without resorting to numerical integration of the governing equations of motion. Specifically, first, an approximate scheme by Cacciola [2010] is employed for deriving an excitation evolutionary power spectrum (EPS) compatible in a stochastic sense with the design spectrum. Note that the choice of utilizing the above scheme is not restrictive, and other alternative approaches for deriving design spectrum compatible power spectra can be adopted. Further, a solution treatment based on a combination of statistical linearization and stochastic averaging is employed that yields an equivalent linear system (ELS) with

4

time-variant stiffness and damping elements. Without loss of generality, systems with softening response behaviors reflecting structural degradation are considered in the ensuing analysis. In this regard, the time instant corresponding to the global minimum and the global maximum of the time-variant stiffness and damping elements, respectively, is treated as the most critical time instant associated with the highest degree of nonlinear/inelastic response behavior exhibited by the structural system. In passing, it is remarked that dos Santos et al. [2016] relied on a somewhat similar concept to develop an efficient stochastic incremental dynamic analysis methodology for circumventing computationally expensive nonlinear system response analyses in a MCS context. Next, the stiffness and damping values at this critical time instant are used in conjunction with the design spectrum for determining approximately the nonlinear system peak response displacement. Note that the peak response estimate is evaluated in an iterative manner till convergence, which ensures that the damping ratio of the imposed design spectrum matches the damping ratio of the ELS.

Compared to earlier relevant efforts in the literature (e.g., Giaralis and Spanos [2010], Mitseas et al. [2018]), the herein developed approach can be construed as an extension to treat structural systems with fractional derivative elements. Furthermore, its significant novel aspect of providing localized time-dependent information via the derived time-variant ELS elements leads to an enhanced accuracy degree when determining nonlinear system peak response estimates. Indeed, it is shown that the values of the ELS stiffness and damping elements at the most critical time instant capture the system dynamics better than an alternative standard statistical linearization solution treatment yielding time-invariant (stationary) ELS stiffness and damping elements (e.g., Giaralis and Spanos [2010], Mitseas et al. [2018]). An illustrative numerical example is considered pertaining to a bilinear hysteretic structural system with fractional derivative elements subject to a Eurocode 8 elastic design spectrum. Comparisons with relevant MCS data are included as well for assessing the accuracy of the approximate approach.

2 Mathematical formulation

2.1 Auxiliary concepts: Equivalent linear system time-dependent damping and stiffness elements, and stochastic averaging solution treatment

The governing equation of motion describing the dynamics of a stochastically excited nonlinear SDOF system with fractional derivative terms takes the form

$$m\ddot{x}(t) + cD_{0,t}^{\alpha}x(t) + g(t, x, \dot{x}) = ma_g(t), \tag{1}$$

where x represents the response displacement process, a dot over a variable denotes differentiation with respect to time t, m is the mass and c is a damping coefficient. Further, $g(t, x, \dot{x})$ is an arbitrary nonlinear function that can account also for hysteretic response behaviors, and $D_{0,t}^{\alpha}x(t)$ denotes the Caputo fractional derivative of order α defined as

$$D_{0,t}^{\alpha}x(t) = \frac{1}{\Gamma(1-\alpha)} \int_0^t \frac{\dot{x}(\tau)}{(t-\tau)^{\alpha}}d\tau, \quad 0 < \alpha < 1, \tag{2}$$

where $\Gamma(\cdot)$ represents the Gamma function. Equivalently, Eq. (1) can be cast in the form

$$\ddot{x}(t) + \beta D_{0,t}^{\alpha}x(t) + g_0(t, x, \dot{x}) = a_g(t), \tag{3}$$

where $\beta = c/m$ and $g_0 = g/m$. Furthermore, $a_g(t)$ is a non-stationary stochastic excitation process with an EPS $S_{a_g}(\omega, t)$ that is compatible with a prescribed design spectrum $S(\omega, \zeta)$, where ω denotes the frequency in rad/s and ζ is the damping ratio.

Note that various approaches have been developed in the literature over the past few decades for deriving stochastic process power spectra that are compatible in a statistical sense with design spectra provided by seismic building codes; see Pfaffinger [1983], Spanos and Loli [1985], Christian [1989], Park [1995], Gupta and Trifunac [1998], Cacciola [2010], Giaralis and Spanos [2009], Shields [2015], Brewick et al. [2018] for some indicative references. Without loss of generality, the approach proposed in Cacciola [2010] is employed in the ensuing analysis for generating $S_{a_g}(\omega, t)$ based on a given $S(\omega, \zeta)$. The salient aspects of the approach are included in A for completeness.

Next, the fundamental ingredients of a recently developed approximate analytical technique for determining the stochastic response of oscillators

governed by Eq. (3) are delineated. The interested reader is also directed to Fragkoulis et al. [2019] for more details. Specifically, relying on a combination of statistical linearization and stochastic averaging (see Roberts and Spanos [1986, 2003] for a broad perspective), the technique in Fragkoulis et al. [2019] yields the non-stationary response amplitude PDF of nonlinear/hysteretic oscillators endowed with fractional derivative elements.

More specifically, considering relatively light damping, the system response exhibits a pseudo-harmonic behavior described by the equations

$$x(t) = A(t)\cos(\omega(A)t + \psi(t)) \tag{4}$$

and

$$\dot{x}(t) = -\omega(A)A(t)\sin(\omega(A)t + \psi(t)), \tag{5}$$

where the response amplitude $A(t)$ and phase $\psi(t)$ are considered to be slowly-varying quantities with respect to time, and thus, approximately constant over one cycle of oscillation. Next, manipulating Eqs. (4) and (5) yields

$$A^2(t) = x^2(t) + \left(\frac{\dot{x}(t)}{\omega(A)}\right)^2. \tag{6}$$

Further, Eq. (3) is recast, equivalently, in the form

$$\ddot{x}(t) + \beta_0\dot{x}(t) + h(t, x, D_{0,t}^\alpha x, \dot{x}) = a_g(t), \tag{7}$$

where

$$h(t, x, D_{0,t}^\alpha x, \dot{x}) = \beta D_{0,t}^\alpha x + g_0(t, x, \dot{x}) - \beta_0\dot{x}, \tag{8}$$

with $\beta_0 = 2\zeta_0\omega_0$ representing a damping coefficient, and ω_0 and ζ_0 denoting, respectively, the natural frequency and damping ratio of the corresponding linear oscillator (i.e., $h(t, x, D_{0,t}^\alpha x, \dot{x}) = \omega_0^2 x(t)$). Furthermore, an ELS is defined as

$$\ddot{x}(t) + (\beta_0 + \beta(A))\dot{x}(t) + \omega^2(A)x(t) = a_g(t). \tag{9}$$

In the following, applying a mean square error minimization between Eqs. (7) and (9), and approximating the involved fractional derivatives according to Spanos et al. [2016], Li et al. [2015], Di Matteo et al. [2018], yields the ELS amplitude-dependent damping and stiffness coefficients in the form [Fragkoulis et al., 2019]

$$\beta(A) = \frac{\omega_0^2}{A\omega(A)}S(A) + \frac{\beta}{\omega^{1-\alpha}(A)}\sin\left(\frac{\alpha\pi}{2}\right) - \beta_0 \tag{10}$$

and

$$\omega^2(A) = \frac{\omega_0^2}{A}F(A) + \beta\omega^\alpha(A)\cos\left(\frac{\alpha\pi}{2}\right), \tag{11}$$

where

$$S(A) = -\frac{1}{\pi}\int_0^{2\pi} g_0(A\cos\phi, -A\omega(A)\sin\phi)\sin\phi\mathrm{d}\phi, \tag{12}$$

$$F(A) = \frac{1}{\pi}\int_0^{2\pi} g_0(A\cos\phi, -A\omega(A)\sin\phi)\cos\phi\mathrm{d}\phi, \tag{13}$$

and $\phi(t) = \omega(A)t + \psi(t)$.

Note that the ELS elements $\omega(A)$ and $\beta(A)$ depend on the response non-stationary amplitude A to account for the nonlinearities and the fractional derivative terms of the original system. Thus, $\omega(A)$ and $\beta(A)$ can be construed as non-stationary stochastic processes, whose time-varying mean values are given by applying the expectation operator on Eqs. (10) and (11). This yields

$$\beta_{eq}(t) = \int_0^\infty \beta(A)p(A,t)\mathrm{d}A \tag{14}$$

and

$$\omega_{eq}^2(t) = \int_0^\infty \omega^2(A)p(A,t)\mathrm{d}A, \tag{15}$$

respectively. Further, Eqs. (14-15) can be associated with an alternative to Eq. (9) ELS of the form

$$\ddot{x}(t) + (\beta_0 + \beta_{eq}(t))\dot{x}(t) + \omega_{eq}^2(t)x(t) = a_g(t). \tag{16}$$

In passing, note that the potent concept of a time-dependent ELS natural frequency, such as the one defined in Eq. (15), has been of considerable importance in the field of structural dynamics. Indicative applications include damage detection (e.g., Spanos et al. [2007]) and identification of moving resonance phenomena (e.g., Beck and Papadimitriou [1993], Tubaldi and Kougioumtzoglou [2015]). The latter can occur, for example, during a seismic event when the decrease of the fundamental system frequency due to yielding tends to track the decrease of the predominant frequency of the ground motion. As a result, nonlinear systems can exhibit significant response amplifications.

Next, it is readily seen that the evaluation of the ELS time-dependent damping $\beta_{eq}(t)$ and stiffness $\omega_{eq}^2(t)$ elements via Eqs. (14-15) requires knowledge of the non-stationary response amplitude PDF $p(A,t)$. In this regard, the stationary response amplitude PDF corresponding to a linear oscillator

8

with fractional derivative terms and subjected to Gaussian white noise was obtained in closed-form in Spanos et al. [2018] based on stochastic averaging. Motivated by this analytical solution, a generalized form of this PDF was considered in Fragkoulis et al. [2019] for modeling the non-stationary response amplitude PDF of the nonlinear oscillator governed by Eq. (3), or equivalently, by Eq. (7). This takes the form

$$p(A, t) = \frac{\sin\left(\frac{\alpha\pi}{2}\right) A}{\omega_0^{1-\alpha} c(t)} \exp\left(\frac{\sin\left(\frac{\alpha\pi}{2}\right)}{\omega_0^{1-\alpha}} \frac{A^2}{2c(t)}\right), \tag{17}$$

where $c(t)$ is a time-dependent coefficient to be determined. Further, based on a stochastic averaging solution treatment of Eq. (16), it was shown in Fragkoulis et al. [2019] that substituting Eq. (17) into the associated Fokker-Planck partial differential equation governing the evolution in time of the response amplitude PDF, i.e.,

$$\frac{\partial p(A, t)}{\partial t} = -\frac{\partial}{\partial A}\left\{\left(-\frac{1}{2}(\beta_0 + \beta_{eq}(t))A + \frac{\pi S_{a_g}(\omega_{eq}(t), t)}{2\omega_{eq}^2(t)A}\right) p(A, t)\right\}$$
$$+ \frac{1}{4}\frac{\partial}{\partial A}\left\{\frac{\pi S_{a_g}(\omega_{eq}(t), t)}{\omega_{eq}^2(t)}\frac{\partial p(A, t)}{\partial A} + \frac{\partial}{\partial A}\left(\frac{\pi S_{a_g}(\omega_{eq}(t), t)}{\omega_{eq}^2(t)}p(A, t)\right)\right\} \tag{18}$$

and manipulating, leads to

$$\dot{c}(t) = -(\beta_0 + \beta_{eq}(c(t)))c(t) + \left(\frac{\sin\left(\frac{\alpha\pi}{2}\right)}{\omega_0^{1-\alpha}}\right)\frac{\pi S_{a_g}(\omega_{eq}(c(t)), t)}{\omega_{eq}^2(c(t))}. \tag{19}$$

Eq. (19) constitutes a deterministic first-order nonlinear ordinary differential equation. This can be solved readily by any standard numerical integration scheme, such as the Runge–Kutta, for determining the time-dependent coefficient $c(t)$. Furthermore, $c(t)$ can be used for evaluating the ELS time-dependent damping and stiffness elements by employing Eqs. (14) and (15). Note that the ELS elements are expressed in Eq. (19) as $\beta_{eq}(t) = \beta_{eq}(c(t))$ and $\omega_{eq}(t) = \omega_{eq}(c(t))$ to highlight the explicit dependence of $\beta_{eq}(t)$ and $\omega_{eq}(t)$ on the time-varying coefficient $c(t)$ via Eqs. (14-15).

It is remarked that various approaches have been proposed in the literature for nonlinear system peak response estimation based on deriving a stationary power spectrum compatible with the provided design spectrum

(e.g., Giaralis and Spanos [2010], Mitseas et al. [2018]). In other words, $a_g(t)$ in Eq. (3) is modeled as a stationary process with a power spectrum $S_{a_g}(\omega)$ compatible with the design spectrum $S(\omega, \zeta)$. In this case, it can be readily seen that employing the technique developed in Fragkoulis et al. [2019] for a stationary excitation process, i.e., $S_{a_g}(\omega, t) = S_{a_g}(\omega)$, leads to a time-invariant stationary PDF for the response amplitude. In fact, Eq. (17) becomes

$$p(A) = \frac{\sin\left(\frac{\alpha\pi}{2}\right) A}{\omega_0^{1-\alpha} c(t_\infty)} \exp\left(\frac{\sin\left(\frac{\alpha\pi}{2}\right)}{\omega_0^{1-\alpha}} \frac{A^2}{2c(t_\infty)}\right), \tag{20}$$

where $c(t_\infty)$ is the stationary constant value of $c(t)$ as $t \to \infty$, and thus, Eqs. (14) and (15) degenerate to

$$\beta_{eq} = \int_0^\infty \beta(A)p(A)\mathrm{d}A \tag{21}$$

and

$$\omega_{eq}^2 = \int_0^\infty \omega(A)p(A)\mathrm{d}A, \tag{22}$$

respectively. Obviously, Eqs. (21-22) represent the stationary mean values of the damping and stiffness elements corresponding to the time-invariant, in this case, ELS of Eq. (16).

2.2 A novel approximate approach for nonlinear system peak response estimation exhibiting enhanced accuracy and accounting for fractional derivative modeling

In this section, a novel approximate approach is developed for determining, in a computationally efficient manner, the peak response of nonlinear structural systems with fractional derivative elements subject to a design spectrum $S(\omega, \zeta)$ provided by seismic building codes. The approach can be construed as an extension of the work in Mitseas et al. [2018] to account for systems with fractional derivative terms. Further, compared to the scheme proposed in Mitseas et al. [2018], the herein developed approach exhibits an enhanced accuracy degree in determining nonlinear system peak response estimates. This is primarily due to the novel aspect of exploiting the localized time-dependent information provided by the derived ELS elements of

Eqs. (14-15). In this regard, the proposed approach is capable of identifying the critical time instant where the nonlinear/inelastic behavior of the system response is most prevalent. Clearly, the values of the ELS elements of Eqs. (14-15) corresponding to this specific time instant capture the localized system dynamics better than the time-invariant (stationary) ELS elements derived in Mitseas et al. [2018] based on a standard statistical linearization treatment. In fact, it is shown that more accurate estimates are obtained for the nonlinear system peak response by employing Eqs. (14-15) compared to their stationary counterparts in Eqs. (21-22).

Specifically, the mechanization of the proposed approach comprises the following steps:

i) Derivation of an excitation EPS $S_{a_g}(\omega, t)$ compatible with the provided elastic design spectrum $S(\omega, \zeta)$; see Cacciola [2010] and A for more details.

ii) Stochastic averaging/linearization solution treatment of the nonlinear/hysteretic oscillator with fractional derivative terms, and determination of ELS time-dependent stiffness $\omega_{eq}(t)$ and damping $\beta_{eq}(t)$ elements via Eqs. (14-15).

iii) Identification of the most critical time instant t_{cr} corresponding to the global maximum and global minimum of $\beta_{eq}(t)$ and $\omega_{eq}(t)$, respectively. This time instant is treated as being associated with the highest degree of nonlinear/inelastic response behavior exhibited by the oscillator.

iv) Evaluation of $\omega_{eq}(t_{cr})$ and $\zeta_{eq}(t_{cr}) = \frac{\beta_0 + \beta_{eq}(t_{cr})}{2\omega_{eq}(t_{cr})}$. If $\frac{|\zeta - \zeta_{eq}(t_{cr})|}{\zeta} < \varepsilon$, then go to step v), otherwise set $\zeta = \zeta_{eq}(t_{cr})$ and repeat steps i)-iv) until convergence. This iterative scheme ensures that the damping ratio of the imposed design spectrum matches the damping ratio of the ELS; see also Mitseas et al. [2018] for more details.

v) Peak response estimation by employing the updated design spectrum $S(\omega, \zeta_{eq}(t_{cr}))$ and considering the ELS natural frequency value $\omega_{eq}(t_{cr})$.

The mechanization of the proposed approach is depicted graphically in Fig. 1, where it is also compared with the original approach in Mitseas et al. [2018]. The novel aspects of the herein developed approach are highlighted in bold red. Clearly, not only the approach in Mitseas et al. [2018] is extended to treat systems with fractional derivative terms, but it also exploits localized

11

time-dependent information for evaluating the ELS elements $\omega_{eq}(t_{cr})$ and $\zeta_{eq}(t_{cr})$. This leads to enhanced accuracy when determining peak response estimates.
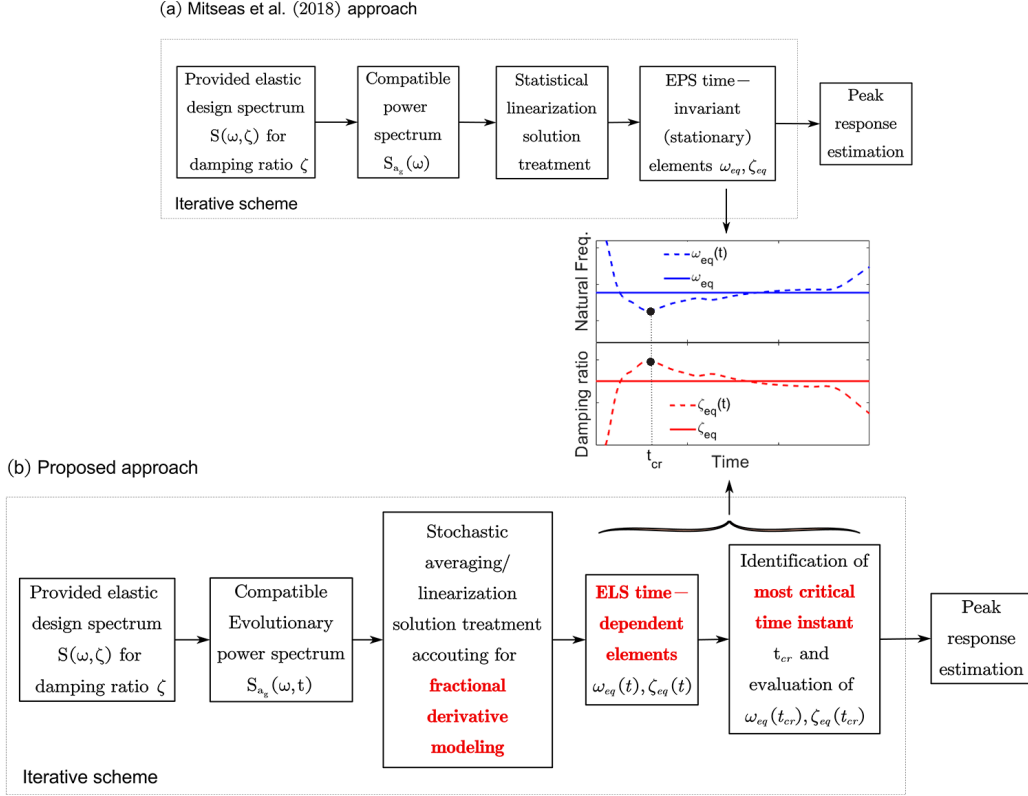

Fig. 1. Nonlinear system peak response estimation: (a) Approach in Mitseas et al. [2018], (b) Proposed approach exhibiting enhanced accuracy and accounting for fractional derivative modeling.

3 Illustrative application

In this section, a bilinear hysteretic structural system with fractional derivative terms subject to a Eurocode 8 elastic design spectrum is considered as an illustrative numerical example for demonstrating the reliability of the developed approach. The achieved accuracy of the predicted peak displacements is quantified by comparison with pertinent results derived from nonlinear re-

sponse history analyses for an ensemble of time-histories compatible with the considered Eurocode 8 design spectrum. B includes details on the definition of the imposed Eurocode 8 elastic design spectrum.

3.1 Governing equations of a bilinear hysteretic structural system with fractional derivative elements, and ELS time-dependent elements

The governing equation of the bilinear hysteretic oscillator, which has been widely utilized in earthquake engineering applications (e.g., Caughey [1960], Roberts and Spanos [2003]), takes the form of Eq.(3) with

$$g_0(t, x, \dot{x}) = \gamma \omega_0^2 x + (1 - \gamma)\omega_0^2 x_y z \tag{23}$$

and

$$x_y \dot{z} = \dot{x}\{1 - H(\dot{x})H(z - 1) - H(-\dot{x})H(-z - 1)\}. \tag{24}$$

In Eqs. (23-24), $H(\cdot)$ denotes the Heaviside step function, γ is the post- to pre-yield stiffness ratio, z is the hysteretic force corresponding to the elasto-plastic characteristic, and x_y is the critical value of the displacement at which the yield occurs.

Next, taking into account Eq. (23), Eqs. (10-11) become (e.g., Fragkoulis et al. [2019])

$$\beta(A) = \frac{(1 - \gamma)\omega_0^2 S(A)}{A\omega(A)} + \frac{\beta}{\omega^{1-\alpha}(A)} \sin\left(\frac{\alpha\pi}{2}\right) - \beta_0 \tag{25}$$

and

$$\omega^2(A) = \omega_0^2 \left[\gamma + \frac{(1 - \gamma)F(A)}{A} + \beta\omega^\alpha(A)\cos\left(\frac{\alpha\pi}{2}\right)\right], \tag{26}$$

respectively, where

$$S(A) = \begin{cases} \frac{4x_y}{\pi}\left(1 - \frac{x_y}{A}\right), & A > x_y \\ 0, & A \le x_y \end{cases} \tag{27}$$

$$F(A) = \begin{cases} \frac{A}{\pi}\left[\Lambda - \frac{1}{2}\sin(2\Lambda)\right], & A > x_y \\ A, & A \le x_y \end{cases} \tag{28}$$

and

$$\cos(\Lambda) = 1 - \frac{2x_y}{A}. \tag{29}$$

13

Further, substituting Eqs. (25) and (26) into Eqs. (14) and (15), respectively, yields

$$
\begin{aligned}
\beta_{eq}(t) = & -\beta_0 + \frac{\beta \sin^2\left(\frac{\alpha\pi}{2}\right)}{\omega_0^{1-\alpha}c(t)} \times \int_0^\infty \frac{A}{\omega^{1-\alpha}(A)} \exp\left(-\frac{\sin\left(\frac{\alpha\pi}{2}\right)}{\omega_0^{1-\alpha}} \frac{A^2}{2c(t)}\right) \mathrm{d}A \\
& + \frac{4x_y\omega_0^2(1-\gamma)\sin\left(\frac{\alpha\pi}{2}\right)}{\pi\omega_0^{1-\alpha}c(t)} \times \int_1^\infty \frac{1-\frac{x_y}{A}}{\omega(A)} \exp\left(-\frac{\sin\left(\frac{\alpha\pi}{2}\right)}{\omega_0^{1-\alpha}} \frac{A^2}{2c(t)}\right) \mathrm{d}A
\end{aligned}
\tag{30}
$$

and

$$
\begin{aligned}
\omega_{eq}^2(t) = & \omega_0^2 - (1-\gamma)\omega_0^2 \left\{ \exp\left(-\frac{x_y{}^2 \sin\left(\frac{\alpha\pi}{2}\right)}{2c(t)\omega_0^{1-\alpha}}\right) - \frac{\sin\left(\frac{\alpha\pi}{2}\right)}{\pi\omega_0^{1-\alpha}c(t)} \right. \\
& \left. \times \int_1^\infty (\Lambda - \frac{1}{2}\sin(2\Lambda))A \times \exp\left(-\frac{\sin\left(\frac{\alpha\pi}{2}\right)}{\omega_0^{1-\alpha}} \frac{A^2}{2c(t)}\right) \mathrm{d}A \right\} \\
& + \frac{\beta \sin\left(\frac{\alpha\pi}{2}\right)\cos\left(\frac{\alpha\pi}{2}\right)}{\omega_0^{1-\alpha}c(t)} \times \int_0^\infty \omega^\alpha(A)A \exp\left(-\frac{\sin\left(\frac{\alpha\pi}{2}\right)}{\omega_0^{1-\alpha}} \frac{A^2}{2c(t)}\right) \mathrm{d}A. \tag{31}
\end{aligned}
$$

3.2 Peak inelastic response determination and comparisons with Monte Carlo simulation data

First, following the approach by Cacciola [2010] described succinctly in A, the excitation EPS $S_{a_g}(\omega, t)$ compatible with the Eurocode 8 design spectrum $S(\omega, \zeta = 0.05)$ (see B) is determined. Specifically, Fig. 2(a) shows the $a_g^R(t)$ component of Eq. (32) referring to a recorded time history at El Centro site of the Imperial Valley earthquake of May 18, 1940. Fig. 2(b) shows a joint time-frequency analysis of the recorded time history at El Centro based on the short-time Thompson's multiple window spectrum estimation scheme proposed in Conte and Peng [1997]. It is readily seen that not only the intensity, but also the frequency content of the time history changes with time. In Fig. 2(c), the power spectrum $G^S(\omega)$ is plotted corresponding to the stationary component $a_g^S(t)$ of Eq. (32). This is determined based on the iterative scheme of Eq. (43). Further, Fig. 2(d) shows the calculated excitation EPS $S_{a_g}(\omega, t)$ compatible with the Eurocode 8 design spectrum. This is used in the ensuing analysis as the input EPS for evaluating the ELS time-dependent elements via Eqs. (30-31). Furthermore, to compare the herein

developed approach shown graphically in Fig. 1(b) with the approach in Mitseas et al. [2018] shown in Fig. 1(a), a design spectrum compatible stationary power spectrum is also determined. Specifically, setting $\alpha = 0$ and $\varphi(t) = 1$ in Eq. (32) yields $S_{a_g}(\omega, t) = S_{a_g}(\omega) = G^S(\omega)$, which is computed based on Eq. (43) and plotted in Fig. 3. Clearly, the $G^S(\omega)$ in Fig. 3 corresponds to a larger variance than the $G^S(\omega)$ in Fig. 2(c). This is anticipated since the additional component of $a_g^R(t)$ in Eq. (32) is omitted in this case, and thus, the intensity of $a_g^S(t)$ needs to increase to counteract the absence of $a_g^R(t)$.
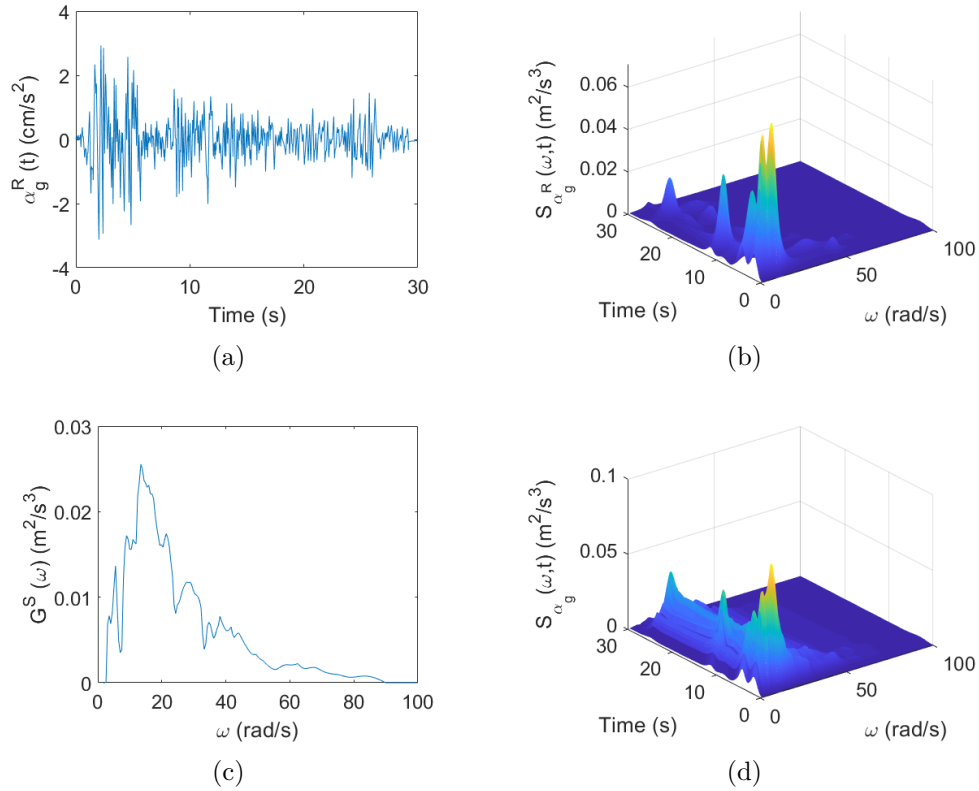

Fig. 2. (a) The recorded time history at El Centro site; (b) EPS estimate of the recorded time history at El Centro site; (c) Calculated power spectrum $G^S(\omega)$ corresponding to the stationary process $a_g^S(t)$; (d) Excitation EPS $S_{a_g}(\omega, t)$ compatible with a Eurocode 8 type B design spectrum $S(\omega, \zeta = 0.05)$.
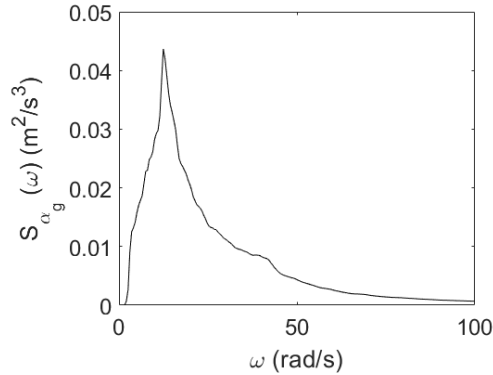
15

Fig. 3. Calculated stationary power spectrum $S_{a_g}(\omega, t) = S_{a_g}(\omega) = G^S(\omega)$ compatible with a Eurocode 8 type B design spectrum $S(\omega, \zeta = 0.05)$.

Further, the parameter values $\omega_0 = 5.48\ rad/sec$, $\beta_0 = 0.7$, $\gamma = 0.4$, $x_y = 7\ cm$ and $\alpha = 0.5$ are used in conjunction with the bilinear hysteretic oscillator with fractional derivative elements described by Eqs. (23-24). The herein developed approach for nonlinear system peak response estimation is applied next. Specifically, considering the excitation EPS in Fig. 2(d) and utilizing Eqs. (30-31), Eq. (19) is solved numerically for $c(t)$. This is substituted into Eqs. (30-31) and the ELS time-variant stiffness $\omega_{eq}(t)$ and damping $\zeta_{eq}(t)$ elements are evaluated. Also, the most critical time instant t_{cr} is identified corresponding to the global minimum and global maximum of $\omega_{eq}(t)$ and $\zeta_{eq}(t)$, respectively.

Next, to ensure that the input design spectrum $S(\omega, \zeta)$ and the ELS of Eq. (16) share the same value of damping ratio ζ, an iterative scheme till convergence is applied, where the design spectrum is updated at each step by setting $S(\omega, \zeta = \zeta_{eq}(t_{cr}))$; see also Mitseas et al. [2018] for more details. In this regard, Fig. 4 shows the computed time-variant elements $\omega_{eq}(t)$ and $\zeta_{eq}(t)$ corresponding to the 4-th iteration when convergence has been reached. These are compared with time-invariant (stationary) elements ω_{eq} and ζ_{eq} obtained by Eqs. (21-22). It is readily seen that $\omega_{eq}(t)$ and $\zeta_{eq}(t)$ are capable of capturing time-localized dynamics of the nonlinear system response. In fact, the value of the ELS natural frequency at the most critical time instant t_{cr}, i.e., $\omega_{eq}(t_{cr})$, is considerably smaller than the time-invariant value ω_{eq}. In other words, $\omega_{eq}(t_{cr})$ reflects a higher degree of nonlinear/inelastic response

behavior than ω_{eq}. In a similar manner, and in agreement with the above argument, $\zeta_{eq}(t_{cr})$ is larger than the time-invariant value ζ_{eq}; thus, reflecting a higher degree of system nonlinearity. Further, the calculated ELS elements $\omega_{eq}(t_{cr})$ and $\zeta_{eq}(t_{cr})$ are plotted in Fig. 4 corresponding to successive iterations of the scheme, and compared with stationary ω_{eq} and ζ_{eq} estimates. It is seen that convergence has been achieved practically after 4 iterations.
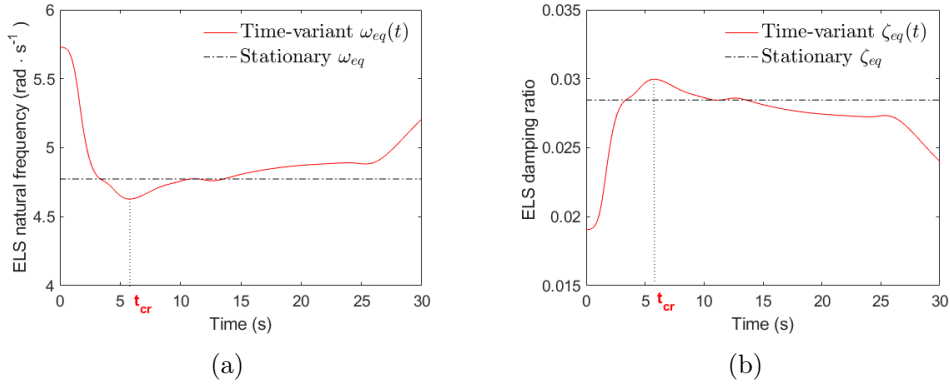

Fig. 4. ELS time-variant elements and most critical time instant t_{cr} based on Eqs. (14-15) and corresponding to the 4-th iteration when convergence of the scheme has been reached: (a) natural frequency $\omega_{eq}(t)$, and (b) damping ratio $\zeta_{eq}(t)$. Comparisons with stationary estimates based on Eqs. (21-22).

Following convergence of the scheme, i.e., $|\zeta - \zeta_{eq}(t_{cr})|/\zeta < \varepsilon$, the obtained ELS elements $\omega_{eq}(t_{cr})$ and $\zeta_{eq}(t_{cr})$ for $k = 4$ in Fig. 5 are used to estimate the nonlinear system peak response in conjunction with the Eurocode 8 elastic design spectrum. This procedure is shown schematically in Fig. 6 where the Eurocode 8 design spectrum is plotted against the natural period $T = 2\pi/\omega$, in terms of spectral acceleration $S(\omega, \zeta_{eq}(t_{cr}))$, left vertical axis, and in terms of spectral displacement $S(\omega, \zeta_{eq}(t_{cr}))/\omega^2$, right vertical axis. Next, the peak inelastic displacement is read on the right vertical axis using the pair $(T_{eq}(t_{cr}) = 2\pi/\omega_{eq}(t_{cr}), \zeta_{eq}(t_{cr}))$ indicated on the figure.

Further, to assess the accuracy of the herein developed approach for nonlinear system peak response estimation, comparisons with pertinent MCS data are included as well. In this regard, an ensemble of 1000 acceleration time-histories are generated compatible with the Eurocode 8 design spectrum $S(\omega, \zeta = 0.05)$ based on Eq. (44) of A. Furthermore, the governing
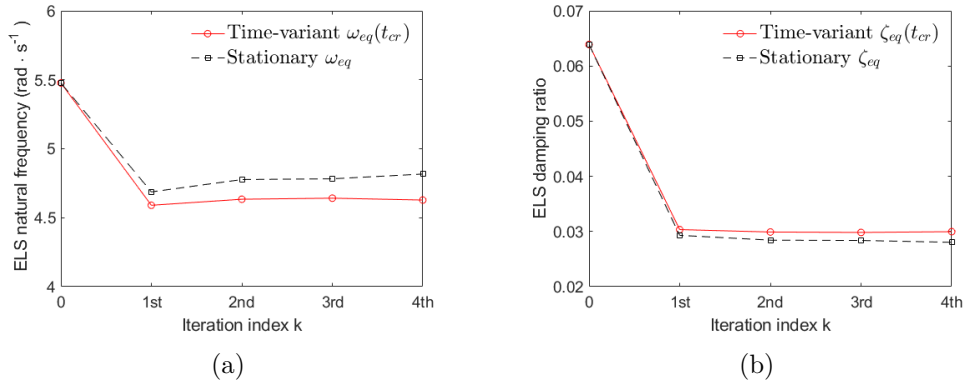
Fig. 5. ELS time-variant elements based on Eqs. (14-15) corresponding to successive iterations and evaluated at the most critical time instant t_{cr}: (a) natural frequency $\omega_{eq}(t_{cr})$, and (b) damping ratio $\zeta_{eq}(t_{cr})$. Comparisons with stationary estimates based on Eqs. (21-22).
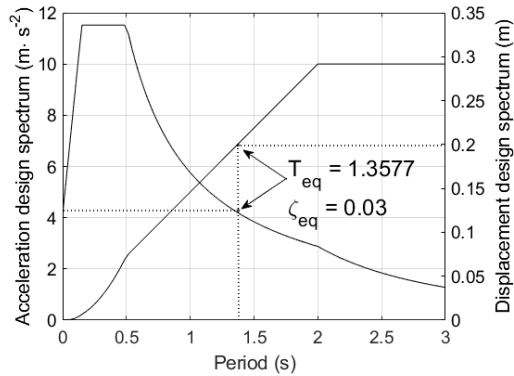

Fig. 6. Nonlinear system peak response displacement determination using the ELS elements $\omega_{eq}(t_{cr})$ and $\zeta_{eq}(t_{cr})$ for $k = 4$ in Fig. 5 in conjunction with the design spectrum of B.

18

Eq. (1) is numerically integrated for the above ensemble by resorting to an L1-algorithm (e.g., Koh and Kelly [1990]), and the mean peak response estimate is obtained based on statistical analysis of the response time-histories. In passing, note that the nonlinearity degree exhibited by the oscillator is significant as shown by the MCS-based average ductility demand estimate. This is calculated as $x_{max}/x_y = 0.1965/0.07 = 2.8$, indicating that the oscillator enters well into the inelastic range.

Table 1 compares the MCS-based estimate with peak displacements obtained by using both the time-variant elements ($\omega_{eq}(t_{cr})$, $\zeta_{eq}(t_{cr})$) and the stationary elements (ω_{eq}, ζ_{eq}), reported in Fig. (5) for $k = 4$, in conjunction with the Eurocode 8 design spectrum as illustrated in Fig. (6). Also, results corresponding to various values of the fractional derivative order α and of the nonlinearity parameter γ are included in Table 1 as well. In all cases, it is seen that the peak response obtained by the proposed approach not only agrees well with the MCS-based estimate, but it also consistently exhibits a higher accuracy degree compared with the results obtained by a stationary treatment of the ELS elements.

Table 1. Peak response displacement of bilinear/hysteretic oscillator with fractional derivative elements using the ELS elements $\omega_{eq}(t_{cr})$ and $\zeta_{eq}(t_{cr})$ for various values of the fractional derivative order α and of the nonlinearity parameter γ. Comparisons with stationary estimates based on Eqs. (21-22), and with MCS data.

Peak displacement estimates					
(α, γ)	MCS	Time-invariant (stationary) elements ω_{eq}, ζ_{eq}	error (based on MCS)	Time-variant elements $\omega_{eq}(t_{cr})$, $\zeta_{eq}(t_{cr})$	error (based on MCS)
$(0.5, 0.4)$	0.1965	0.1939	1.3%	0.1977	0.6%
$(0.75, 0.4)$	0.1623	0.1587	2.2%	0.1618	0.3%
$(0.5, 0.2)$	0.1941	0.1852	4.6%	0.1901	2.1%
$(0.75, 0.2)$	0.1675	0.1585	5.4%	0.1630	2.7%

19

4 Concluding remarks

In this paper, an approximate approach has been developed for determining the peak response displacement of nonlinear structural systems with fractional derivative elements subject to a given seismic design spectrum. This has been done in a computationally efficient manner without resorting to numerical integration of the governing equations of motion. Specifically, first, an approximate scheme has been utilized for deriving an excitation EPS compatible in a stochastic sense with the design spectrum. Further, employing a solution treatment based on a combination of statistical linearization and stochastic averaging has yielded an ELS with time-variant stiffness and damping elements. Without loss of generality, systems with softening response behaviors reflecting structural degradation have been considered. In this setting, it has been shown that the global minimum and the global maximum of the time-variant stiffness and damping elements, respectively, correspond to the time instant associated with the highest degree of nonlinear/inelastic response behavior exhibited by the oscillator. In this regard, the stiffness and damping values at this critical time instant have been used in conjunction with the design spectrum for determining approximately the nonlinear oscillator peak response displacement. Compared to earlier relevant efforts in the literature (e.g., Giaralis and Spanos [2010], Mitseas et al. [2018]), the herein developed approach can be construed as an extension to treat systems with fractional derivative elements. Furthermore, its significant novel aspect of providing localized time-dependent information via the derived time-variant ELS elements leads to an enhanced accuracy degree when determining nonlinear system peak response estimates. Indeed, it has been shown that the values of the ELS stiffness and damping elements at the most critical time instant capture the system dynamics better than an alternative standard statistical linearization solution treatment yielding time-invariant (stationary) ELS stiffness and damping elements. An illustrative numerical example has been considered for assessing the performance of the approximate approach, pertaining to a bilinear hysteretic oscillator with fractional derivative elements subject to a Eurocode 8 elastic design spectrum. Comparisons with relevant Monte Carlo simulation data have demonstrated a high degree of accuracy.

Acknowledgment

A Derivation of design spectrum compatible excitation evolutionary power spectrum

Following Cacciola [2010], the non-stationary excitation stochastic process $a_g(t)$ comprises a fully non-stationary component $a_g^R(t)$ modeled by a recorded earthquake time-history, and a time-modulated stationary zero-mean Gaussian process $a_g^S(t)$, i.e.,

$$a_g(t) = \alpha a_g^R(t) + \varphi(t) a_g^S(t). \tag{32}$$

In Eq. (32), both the scaling factor α and the power spectrum $G^S(\omega)$ of the stationary process $a_g^S(t)$ are unknowns to be determined, and the time-modulating function $\varphi(t)$ is given as

$$\varphi(t) = \begin{cases} \left(\frac{t}{t_1}\right)^2, & t < t_1 \\ 1, & t_1 \leq t \leq t_2 \\ \exp\left[-\beta(t - t_2)\right], & t > t_2 \end{cases} \tag{33}$$

where $t_2 = t_1 + T_s$, with T_s representing the time window during which stationarity is assumed. Next, an approximate relationship can be derived for the corresponding design spectra; that is,

$$S(\omega, \zeta) = \sqrt{\alpha^2 S^R(\omega, \zeta)^2 + S^S(\omega, \zeta)^2}, \tag{34}$$

where $S^R(\omega, \zeta)$ and $S^S(\omega, \zeta)$ are the design spectra referring to the response a linear oscillator subject to $a_g^R(t)$ and $a_g^S(t)$, respectively. Taking into account Eq. (34), the value of α lies in the range $(0, 1]$ and is estimated as

$$\alpha = \min\left\{\frac{S(\omega, \zeta)}{S^R(\omega, \zeta)}\right\}. \tag{35}$$

21

Next, attention is directed to determining $G^S(\omega)$. This is done by relying on an approximate solution treatment of the first-passage time problem according to Vanmarcke [1976], and to an iterative scheme proposed by Cacciola et al. [2004]. Specifically, consider the n-th order stationary response spectral moment of a linear SDOF oscillator

$$\lambda_n = \int_0^\infty \omega^n \frac{1}{(\omega_0^2 - \omega^2)^2 + (2\zeta_0\omega_0\omega)^2} G^S(\omega)\mathrm{d}\omega, \tag{36}$$

where ω_0 and ζ_0 are the natural frequency and the damping ratio of the oscillator. Further, assuming a sufficiently long duration of $T_s \geq 15 \ s$, $G^S(\omega)$ can be related to $S^S(\omega_0, \zeta_0)$ in a statistical manner via the concept of the "peak factor" η. That is,

$$S^S(\omega_0, \zeta_0) = \omega_0^2 \eta \sqrt{\lambda_0(\omega_0, \zeta)}, \tag{37}$$

where the peak factor can be estimated by the semi-empirical expression [Vanmarcke, 1976]

$$\eta = \sqrt{2\ln(2\mu)\left[1 - \exp\left(-\delta\sqrt{\pi\ln(2\mu)}\right)\right]}. \tag{38}$$

In Eq. (38), the mean zero crossing rate μ and the spread factor δ are defined as

$$\mu = \frac{T_s}{2\pi}\sqrt{\frac{\lambda_2}{\lambda_0}}(-\ln p)^{-1}, \tag{39}$$

and

$$\delta = \sqrt{1 - \frac{\lambda_1^2}{\lambda_0\lambda_2}}, \tag{40}$$

respectively. Herein, the probability p in Eq. (39) is set equal to 0.5, so that $S^S(\omega_0, \zeta_0)$ in Eq. (37) is interpreted as the "median" pseudo-acceleration design spectrum. That is, half of the displacement response spectral ordinates of an ensemble of stationary samples of duration T_s compatible with the power spectrum $G^S(\omega)$ lie below $S^S(\omega_0, \zeta_0)/\omega_0^2$; see also Giaralis and Spanos [2010] and Mitseas et al. [2018] for more details. Next, relying on the approximate expression [Vanmarcke, 1976]

$$\lambda_0 = \frac{G^S(\omega_0)}{\omega_0^3}\left(\frac{\pi}{4\zeta_0} - 1\right) + \frac{1}{\omega_0^4}\int_0^{\omega_i} G^S(\omega)\mathrm{d}\omega, \tag{41}$$

substituting Eq. (41) into Eq. (37), and manipulating, yields

$$S^S(\omega_0, \zeta_0) = \eta^2 \omega_0 G^S(\omega_0)\left(\frac{4 - \pi\zeta_0}{4\zeta_0}\right) + \eta^2 \int_0^{\omega_i} G^S(\omega)\mathrm{d}\omega. \qquad (42)$$

Applying a discretization of the frequency domain into a uniform grid of M frequency points $\omega_i = \omega_b^l + (i - 0.5)\Delta\omega$, $i = 1, 2, \ldots, M$ within the range (ω_b^l, ω_b^u), and manipulating Eq. (42), yields [Cacciola et al., 2004]

$$G^S(\omega_i) = \begin{cases} \frac{4\zeta}{\omega_i\pi - 4\zeta_0\omega_{i-1}}\left(\frac{(S^S(\omega_0, \zeta_0))^2}{\eta^2} - \Delta\omega\sum_{q=1}^{i-1}G^S(\omega_q)\right), & \omega_b^l < \omega_i < \omega_b^u \\ 0, & \omega_i \le \omega_b^l \end{cases} \qquad (43)$$

Eq. (43) can be recursively applied for $i = 1, 2, \ldots, M$ to evaluate the ordinates of the power spectrum $G^S(\omega)$ at the M frequency points ω_i lying $\delta\omega$ apart in the range (ω_b^l, ω_b^u).

Further, following determination of $G^S(\omega)$, a k-th non-stationary acceleration time-history can be generated based on spectral representation theory (e.g., Shinozuka and Deodatis [1991], Liang et al. [2007]). That is,

$$a_g^{(k)}(t) = \alpha a_g^R(t) + \varphi(t)\sum_{i=1}^{N_a}\sqrt{4G^S(i\Delta\omega)\Delta\omega}\cos\left(i\Delta\omega t + \phi_i^{(k)}\right), \qquad (44)$$

where $\phi_i^{(k)}$ are independent random phases uniformly distributed in the interval $[0, 2\pi)$, and N_a is the number of harmonics to be considered in the summation. Clearly, the non-separable EPS $S_{a_g}(\omega, t)$ can be estimated by various joint time-frequency analysis techniques based on statistical analysis of an ensemble of realizations generated by Eq. (44) (e.g., Qian [2002], Spanos and Failla [2004], Kougioumtzoglou et al. [2012, 2020]). Furthermore, iterative improvement of the $G^S(\omega)$ may be required for satisfying code provisions. To this aim, the iterative scheme

$$G^{S(j)}(\omega) = G^{S(j-1)}(\omega)\left(\frac{S(\omega, \zeta)^2}{\hat{S}^{(j-1)}(\omega, \zeta)^2}\right), \qquad (45)$$

can be applied, where $\hat{S}^{(j-1)}(\omega, \zeta)^2$ is the mean design spectrum of the ground acceleration $a_g(t)$ at the $(j - 1)$-th iteration; see also Cacciola [2010] and references therein for more details.

Note that the approach presented succinctly in this Appendix degenerates to the scheme in Cacciola et al. [2004] by setting $\alpha = 0$ and $\varphi(t) = 1$ in Eq. (32). In this regard, the design spectrum compatible power spectrum becomes $S_{a_g}(\omega, t) = G^S(\omega)$ corresponding to the stationary process $a_g^S(t)$.

B Eurocode 8 design spectrum

The Eurocode 8 design spectrum for peak ground acceleration $0.36g$ ($g = 981\ cm/s^2$) and ground type B used in the numerical example of this paper is defined as [CEN, 2004]

$$S(T, \zeta) = 0.432g \times \begin{cases} 1 + \frac{T}{0.15}(2.5\delta - 1), & 0 \leq T \leq 0.15 \\ 2.5\delta, & 0.15 \leq T \leq 0.5 \\ \frac{1.25\delta}{T}, & 0.5 \leq T \leq 2 \\ \frac{2.5\delta}{T^2}, & 2 \leq T \leq 4 \end{cases} \tag{46}$$

where

$$\delta = \sqrt{\frac{10}{5 + \zeta}} \geq 0.55, \tag{47}$$

$T = 2\pi/\omega$ is the natural period and ζ is the damping ratio.

References

Anil K Chopra. Dynamics of structures. Theory and applications to earthquake engineering, 2nd edition. New Jersey, Prentice-Hall, 2001.

Yu-Yuan Lin, Eduardo Miranda, and Kuo-Chun Chang. Evaluation of damping reduction factors for estimating elastic response of structures with high damping. Earthquake engineering & structural dynamics, 34(11):1427–1443, 2005.

CEN. Eurocode 8: Design of Structures for Earthquake Resistance - Part 1: General Rules, Seismic Actions and Rules for Buildings. Comité Européen de Normalisation, Brussels, EN 1998-1: 2003 E., 2004.

Evangelos I Katsanos, Anastasios G Sextos, and George D Manolis. Selection of earthquake ground motion records: A state-of-the-art review from a structural engineering perspective. Soil dynamics and earthquake engineering, 30(4):157–169, 2010.

A Giaralis and PD Spanos. Wavelet-based response spectrum compatible synthesis of accelerograms—eurocode application (EC8). Soil Dynamics and Earthquake Engineering, 29(1):219–235, 2009.

Pierfrancesco Cacciola. A stochastic approach for generating spectrum compatible fully nonstationary earthquakes. Computers & Structures, 88(15-16):889–901, 2010.

Miguel Araújo, Luís Macedo, Mário Marques, and José Miguel Castro. Code-based record selection methods for seismic performance assessment of buildings. Earthquake Engineering & Structural Dynamics, 45(1):129–148, 2016.

Mircea Grigoriu. To scale or not to scale seismic ground-acceleration records. Journal of engineering mechanics, 137(4):284–293, 2011.

Katrin Beyer and Julian J Bommer. Selection and scaling of real accelerograms for bi-directional loading: a review of current practice and code provisions. Journal of earthquake engineering, 11(S1):13–45, 2007.

Nicos Makris. Three-dimensional constitutive viscoelastic laws with fractional order time derivatives. Journal of Rheology, 41(5):1007–1020, 1997.

J A T M J Sabatier, Ohm Parkash Agrawal, and J A Tenreiro Machado. Advances in fractional calculus, volume 4. Springer, 2007.

Yuriy A Rossikhin and Marina V Shitikova. Application of fractional calculus for dynamic problems of solid mechanics: novel trends and recent results. Applied Mechanics Reviews, 63(1), 2010.

Mario Di Paola, Giuseppe Failla, Antonina Pirrotta, Alba Sofi, and Massimiliano Zingales. The mechanically based non-local elasticity: an overview of main results and future challenges. Philosophical Transactions of the Royal Society A: Mathematical, Physical and Engineering Sciences, 371 (1993):20120433, 2013.

Mi Di Paola, A Pirrotta, and A Valenza. Visco-elastic behavior through fractional calculus: an easier method for best fitting experimental results. Mechanics of materials, 43(12):799–806, 2011.

Chan Ghee Koh and James M Kelly. Application of fractional derivatives to seismic analysis of base-isolated models. Earthquake engineering & structural dynamics, 19(2):229–241, 1990.

Nicos Makris and M C Constantinou. Fractional-derivative maxwell model for viscous dampers. Journal of Structural Engineering, 117(9):2708–2724, 1991.

H H Lee and C-S Tsai. Analytical model of viscoelastic dampers for seismic mitigation of structures. Computers & structures, 50(1):111–121, 1994.

K L Shen and T T Soong. Modeling of viscoelastic dampers for structural applications. Journal of Engineering Mechanics, 121(6):694–701, 1995.

Finn Rüdinger. Tuned mass damper with fractional derivative damping. Engineering Structures, 28(13):1774–1779, 2006.

Ioannis Petromichelakis, Apostolos F Psaros, and Ioannis A Kougioumtzoglou. Stochastic response analysis and reliability-based design optimization of nonlinear electromechanical energy harvesters with fractional derivative elements. ASCE-ASME J Risk and Uncert in Engrg Sys Part B Mech Engrg, 7(1), 2021.

Pol D Spanos and Georgios I Evangelatos. Response of a non-linear system with restoring forces governed by fractional derivatives—time domain simulation and statistical linearization solution. Soil Dynamics and Earthquake Engineering, 30(9):811–821, 2010.

Alberto Di Matteo, Ioannis A Kougioumtzoglou, Antonina Pirrotta, Pol D Spanos, and Mario Di Paola. Stochastic response determination of nonlinear oscillators with fractional derivatives elements via the Wiener path integral. Probabilistic Engineering Mechanics, 38:127–135, 2014.

V C Fragkoulis, I A Kougioumtzoglou, A A Pantelous, and M Beer. Non-stationary response statistics of nonlinear oscillators with fractional derivative elements under evolutionary stochastic excitation. Nonlinear Dynamics, 97(4):2291–2303, 2019.

A Pirrotta, I A Kougioumtzoglou, A Di Matteo, V C Fragkoulis, A A Pantelous, and C Adam. Deterministic and random vibration of linear systems with singular parameter matrices and fractional derivative terms. Journal of Engineering Mechanics, 147(6):04021031, 2021.

Fan Kong, Yixin Zhang, and Yuanjin Zhang. Non-stationary response power spectrum determination of linear/non-linear systems endowed with fractional derivative elements via harmonic wavelet. Mechanical Systems and Signal Processing, 162:108024, 2022a.

Fan Kong, Renjie Han, and Yuanjin Zhang. Approximate stochastic response of hysteretic system with fractional element and subjected to combined stochastic and periodic excitation. Nonlinear Dynamics, 107(1):375–390, 2022b.

W D Iwan. Estimating inelastic response spectra from elastic spectra. Earthquake Engineering & Structural Dynamics, 8(4):375–388, 1980.

Wilfred D Iwan and Nathan C Gates. Estimating earthquake response of simple hysteretic structures. Journal of the Engineering Mechanics Division, 105(3):391–405, 1979a.

Paul C Jennings. Equivalent viscous damping for yielding structures. Journal of the Engineering Mechanics Division, 94(1):103–116, 1968.

Wilfred D Iwan and Nathan C Gates. The effective period and damping of a class of hysteretic structures. Earthquake Engineering & Structural Dynamics, 7(3):199–211, 1979b.

A H Hadjian. A re-evaluation of equivalent linear models for simple yielding systems. Earthquake Engineering & Structural Dynamics, 10(6):759–767, 1982.

PK Koliopulos, EA Nichol, and GD Stefanou. Comparative performance of equivalent linearization techniques for inelastic seismic design. Engineering Structures, 16(1):5–10, 1994.

Agathoklis Giaralis and Pol D Spanos. Effective linear damping and stiffness coefficients of nonlinear systems for design spectrum based analysis. Soil Dynamics and Earthquake Engineering, 30(9):798–810, 2010.

Ioannis P Mitseas, Ioannis A Kougioumtzoglou, Agathoklis Giaralis, and Michael Beer. A novel stochastic linearization framework for seismic demand estimation of hysteretic MDOF systems subject to linear response spectra. Structural Safety, 72:84–98, 2018.

Ioannis P Mitseas and Michael Beer. Modal decomposition method for response spectrum based analysis of nonlinear and non-classically damped systems. Mechanical Systems and Signal Processing, 131:469–485, 2019.

Ketson RM dos Santos, Ioannis A Kougioumtzoglou, and André T Beck. Incremental dynamic analysis: a nonlinear stochastic dynamics perspective. Journal of Engineering Mechanics, 142(10):06016007, 2016.

Dieter D Pfaffinger. Calculation of power spectra from response spectra. Journal of Engineering Mechanics, 109(1):357–372, 1983.

P D Spanos and L M Vargas Loli. A statistical approach to generation of design spectrum compatible earthquake time histories. International Journal of Soil Dynamics and Earthquake Engineering, 4(1):2–8, 1985.

John T Christian. Generating seismic design power spectral density functions. Earthquake spectra, 5(2):351–368, 1989.

Young J Park. New conversion method from response spectrum to PSD functions. Journal of Engineering Mechanics, 121(12):1391–1392, 1995.

I D Gupta and M D Trifunac. Defining equivalent stationary PSDF to account for nonstationarity of earthquake ground motion. Soil Dynamics and Earthquake Engineering, 17(2):89–99, 1998.

MD Shields. Simulation of spatially correlated nonstationary response spectrum–compatible ground motion time histories. Journal of Engineering Mechanics, 141(6):04014161, 2015.

Patrick T Brewick, Miguel Hernandez-Garcia, Sami F Masri, and Andrew W Smyth. A data-based probabilistic approach for the generation of spectra-compatible time-history records. Journal of Earthquake Engineering, 22 (8):1365–1391, 2018.

J B Roberts and P D Spanos. Stochastic averaging: an approximate method of solving random vibration problems. International Journal of Non-Linear Mechanics, 21(2):111–134, 1986.

John Brian Roberts and Pol D Spanos. Random vibration and statistical linearization. Courier Corporation, 2003.

Pol D Spanos, Alberto Di Matteo, Yezeng Cheng, Antonina Pirrotta, and Jie Li. Galerkin scheme-based determination of survival probability of oscillators with fractional derivative elements. Journal of Applied Mechanics, 83(12), 2016.

Wei Li, Lincong Chen, Natasa Trisovic, Aleksandar Cvetkovic, and Junfeng Zhao. First passage of stochastic fractional derivative systems with power-form restoring force. International Journal of Non-Linear Mechanics, 71: 83–88, 2015.

A Di Matteo, P D Spanos, and A Pirrotta. Approximate survival probability determination of hysteretic systems with fractional derivative elements. Probabilistic Engineering Mechanics, 54:138–146, 2018.

Pol D Spanos, Agathoklis Giaralis, Nikolaos P Politis, and Jose M Roesset. Numerical treatment of seismic accelerograms and of inelastic seismic structural responses using harmonic wavelets. Computer-Aided Civil and Infrastructure Engineering, 22(4):254–264, 2007.

J L Beck and C Papadimitriou. Moving resonance in nonlinear response to fully nonstationary stochastic ground motion. Probabilistic Engineering Mechanics, 8(3-4):157–167, 1993.

Enrico Tubaldi and Ioannis A Kougioumtzoglou. Nonstationary stochastic response of structural systems equipped with nonlinear viscous dampers under seismic excitation. Earthquake Engineering & Structural Dynamics, 44(1):121–138, 2015.

Pol D Spanos, Ioannis A Kougioumtzoglou, Ketson RM dos Santos, and André T Beck. Stochastic averaging of nonlinear oscillators: Hilbert transform perspective. Journal of Engineering Mechanics, 144(2):04017173, 2018.

T K Caughey. Random excitation of a system with bilinear hysteresis. J. Appl. Mech., 27(4):649–652, 1960.

J P Conte and B F Peng. Fully nonstationary analytical earthquake ground-motion model. Journal of Engineering Mechanics, 123(1):15–24, 1997.

Erik H Vanmarcke. Structural response to earthquakes. In Developments in Geotechnical Engineering, volume 15, pages 287–337. Elsevier, 1976.

Pierfrancesco Cacciola, P Colajanni, and G Muscolino. Combination of modal responses consistent with seismic input representation. Journal of Structural Engineering, 130(1):47–55, 2004.

Masanobu Shinozuka and George Deodatis. Simulation of stochastic processes by spectral representation. Applied Mechanics Reviews, 44(4):191–204, 04 1991.

Jianwen Liang, Samit Ray Chaudhuri, and Masanobu Shinozuka. Simulation of nonstationary stochastic processes by spectral representation. Journal of Engineering Mechanics, 133(6):616–627, 2007.

Shie Qian. Introduction to time-frequency and wavelet transforms, volume 68. Prentice Hall PTR Upper Saddle River (NJ), 2002.

Pol D Spanos and Giuseppe Failla. Evolutionary spectra estimation using wavelets. Journal of Engineering Mechanics, 130(8):952–960, 2004.

Ioannis A Kougioumtzoglou, Fan Kong, Pol D Spanos, and Jie Li. Some observations on wavelets based evolutionary power spectrum estimation. In Proceedings of the stochastic mechanics conference (SM12), Ustica, Italy, volume 3, pages 37–44, 2012.

Ioannis A Kougioumtzoglou, Ioannis Petromichelakis, and Apostolos F Psaros. Sparse representations and compressive sampling approaches in engineering mechanics: A review of theoretical concepts and diverse applications. Probabilistic Engineering Mechanics, 61:103082, 2020.